polymers[19,20] and whether assignment to the amorphous fraction is appropriate. The mechanical studies were not able to address this since the introduction of the epoxy groups had only a minor effect on the measured characteristics of the process. However, in the dielectric case, which responds specifically to the introduction of polar groups, the effect is pronounced. A subglass process that can be well characterized is now observed. In view of the fact that the epoxidation only alters the chemical structure of the surface and not its organization, at the very least it may be said that the amorphous overlayer in single-crystal lamellas is the location of a well-developed subglass relaxation process. This has not been an easy phenomenon to demonstrate experimentally, and the epoxidized specimens constitute an ideal system for accomplishing this.

Solution crystallization of the surface reacted lamellas under the conditions used in this work yields multilamellar structures with cores of α-TPI and noncrystalline traverses containing blocks of TPI and epoxidized TPI, as described above. The lengths of the noncrystalline traverses are distributed about two or more different values due to the exclusion of complete blocks of TPI or epoxidized TPI units from the crystal core. The change in morphology upon copolymer crystallization is accompanied by a shift of the primary dielectric process to lower temperatures without a significant change in the activation energy, suggesting some relaxation of restraints on the chain sections involved with little change in the energy barriers to motion. The secondary process for the segmented block copolymer appears to be less sensitive to the change in morphology which again suggests that a localized motion is involved for both preparations.[19]

Acknowledgment is made to the PSC/CUNY faculty research program for support of part of this research. F.L. and R.H.B. are grateful to the National Science Foundation Polymers Program for financial support (DMR 86-16565).

Registry No. TPI, 9003-31-0.

References and Notes

(1) Schlesinger, W.; Leeper, H. M. *J. Polym. Sci.* **1953**, *11*, 203.
(2) Keller, A.; Martuscelli, E. *Makromol. Chem.* **1972**, *151*, 189.
(3) Anandakumaran, K.; Kuo, C.-C.; Mukherji, S.; Woodward, A. E. *J. Polym. Sci., Polym. Phys. Ed.* **1982**, *20*, 1669.
(4) Anandakumaran, K.; Herman, W.; Woodward, A. E. *Macromolecules* **1983**, *16*, 563.
(5) Kuo, C.-C.; Woodward, A. E. *Macromolecules* **1984**, *17*, 1034.
(6) Xu, J.; Woodward, A. E. *Macromolecules* **1986**, *19*, 1114.
(7) Corrigan, J. P.; Zemel, I. S.; Woodward, A. E. *J. Polym. Sci., Polym. Phys. Ed.* **1989**, *27*, 1135.
(8) Xu, J.; Woodward, A. E. *Macromolecules* **1988**, *21*, 83.
(9) Gavish, M.; Corrigan, J.; Woodward, A. E. *Macromolecules* **1988**, *21*, 2079.
(10) Anandakumaran, K.; St. John Manley, R. *J. Polym. Sci., Polym. Phys. Ed.* **1989**, *27*, 1425.
(11) Schilling, F. C.; Bovey, F. A.; Anandakumaran, K.; Woodward, A. E. *Macromolecules* **1985**, *18*, 2688.
(12) Tischler, F.; Woodward, A. E. *Macromolecules* **1986**, *19*, 1328.
(13) Zemel, I. S.; Corrigan, J. P.; Woodward, A. E. *J. Polym. Sci., Polym. Phys. Ed.* **1989**, *27*, 2479.
(14) Kakizaki, M.; Hideshima, T. *J. Macromol. Sci., Phys.* **1973**, *B8*, 367.
(15) North, A. M.; Reid, J. C. *Eur. Polym. J.* **1972**, *8*, 1129.
(16) Mopsik, F. I. *Rev. Sci. Instrum.* **1984**, *55*, 79.
(17) Mopsik, F. I. *IEEE Trans. Electr. Insul.* **1985**, *EI-20*, 957.
(18) This configuration was suggested to us: Mopsik, R. I., private communication.
(19) McCrum, N. G.; Williams, G.; Read, B. E. *Anelastic and Dielectric Effects in Polymeric Solids*; Wiley: New York, 1967.
(20) Boyd, R. H. *Polymer* **1985**, *26*, 323.
(21) Cooper, W.; Vaugh, G. *Polymer* **1963**, *4*, 329.
(22) Nelson, R. D., Jr.; Lide, D. R., Jr.; Maryott, A. A. *Natl. Stand. Ref. Data Series (U.S., Natl. Bur. Stand.)* **1967**, *NSRDS-NBS 10*.

Monte Carlo Studies of the Interface between Two Polymer Melts

Johannes Reiter, Gerhard Zifferer, and Oskar Friedrich Olaj*

Institut für Physikalische Chemie, Universität Wien, Währingerstrasse 42, A-1090 Wien, Austria. *Received November 15, 1988; Revised Manuscript Received June 1, 1989*

ABSTRACT: By use of pseudokinetic rearrangements, the interface between two polymer melts that are mutually repulsive but otherwise identical is simulated on a five-way cubic lattice at a total volume fraction of unity. The position of the interface, which has been deliberately located at $z = 0$, remains stable if the repulsion energy is large enough and if it is ensured in the algorithm that the ratio of the volume fractions of the two polymers is distributed sharply about unity. Conventional periodic boundary conditions were used in the x and y direction, while antiperiodic boundary conditions were introduced at $z = -l_z/2$ and $z = +l_z/2$ (l_z being the lattice dimension in the z direction). At such an antiperiodic boundary one kind of chain is continued as the other kind if the chain stretches across that boundary and nearest neighbors are counted as the same if they are different (and as different if they are the same), thus avoiding the need for a hard boundary. The interface appears to be thicker and local energies are lower than predicted by mean field theories. At the interface it is seen that chain ends and, in case of polydisperse polymers, smaller chains migrate preferentially into the opposite melt while chain dimensions perpendicular to the interface are decreased.

1. Introduction

Although there is considerable interest in the behavior of macromolecules at interfaces there have been only a few Monte Carlo studies on bulk polymers near interfaces. These investigations have recently been summarized by Madden[1] who simulated the melt–vapor interface of a polymer with a combination of pseudokinetic

0024-9297/90/2223-0224$02.50/0

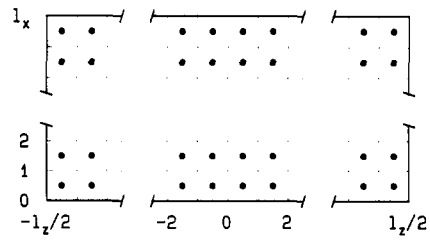

Figure 1. Cross section (parallel to the x/z or y/z plane) of a rectangular portion of the five-way cubic lattice with dimensions (l_x, l_y, l_z). The positions of segments are indicated by ●.

rearrangements and microrelaxations at a volume fraction less than unity. Here we want to study the interface between two immiscible bulk polymers, subjecting them to pseudokinetic rearrangements at a volume fraction of unity.

2. Model and Simulation Method

The subject of our study is a polymer system consisting of linear chains of (average) length $\langle N \rangle = 100$ covering a rectangular section of a five-way cubic lattice with the dimensions (l_x, l_y, l_z) = (25, 25, 48) at a polymer volume fraction of unity. x and y range from 0 to l_x and from 0 to l_y, respectively, while z goes from $-l_z/2$ to $+l_z/2$, the segments occupying points with coordinates of integer ± 0.5. The situation is schematically depicted in Figure 1.

General Outline of the Procedure. Initially the system is equilibrated; all the chains are treated as being of the same kind and periodic boundary conditions are used in all three dimensions. Then all polymers with a negative z component of their center of mass position are taken to be kind A and the others (with a positive z component) to be kind B. Now $E_{AB} = \epsilon_{AB}/kT$, the reduced interaction energy between a segment of the one kind and a nearest-neighbor segment of the other kind, is set to its final (nonzero and positive) value, which is more repulsive than the decomposition energy. Simultaneously, we convert the *periodic* boundary conditions at $z = -l_z/2$ and $z = +l_z/2$ to *antiperiodic* boundary conditions: Due to the symmetry of the system, A chains left of the interface are formally indistinguishable from B chains right of the interface and vice versa. As a consequence, (a) A chains can be continued as B chains and vice versa if they cross the antiperiodic boundary and (b) nearest neighbor segments are counted as the same if they are different (and as different if they are the same) if the interaction is across that boundary. Finally, the simulation is continued with the interface located at $z = 0$, using the pseudokinetic rearrangements introduced by Olaj et al.[2,3] and Mansfield.[4] These are schematically represented in Figure 2. They comprise for intermolecular rearrangements[3] dimerization with successive cleavage (a), substitution (b), and the metathesis (bond flip) reaction (c) and, in addition, for intramolecular reactions the backbite reaction[4] (d) and cyclization with successive cleavage[1] (e). Unfortunately, the intermolecular reactions may change the distribution of chain lengths and alter the ratio of A segments to B segments. As for the former, we allow only reactions that either yield chain lengths within the interval INT($\langle N \rangle$[1 ± 0.5]) (constraint I, where $\langle N \rangle$ is the number average chain length) or are bound to yield a narrow distribution about $\langle N \rangle$, the width of which is controlled by a distribution-narrowing parameter f, as proposed by Olaj and Lantschbauer[3] (constraint II). As for the latter, if the two reacting chains are of different kind, we randomly

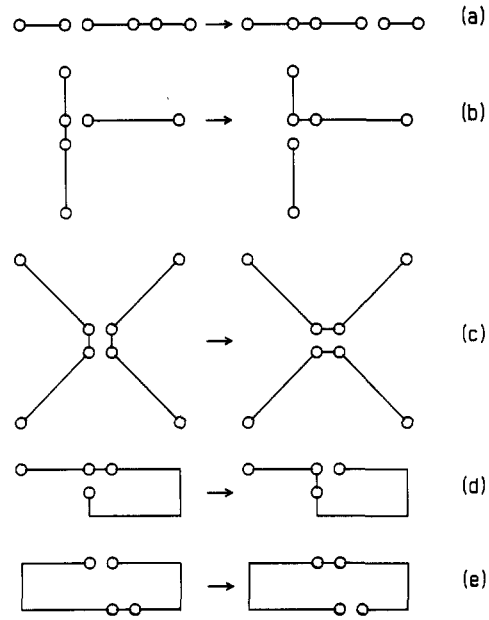

Figure 2. Schematic representation of the (rearrangement) processes used for chain relaxation:[1-4] Dimerization with successive cleavage (a); substitution reaction (b); metathesis (bond flip) reaction (c); backbite reaction (d); cyclization with successive cleavage (e).

assign one as type A and one as type B. The volume fraction of A (or B) segments then is forced to be Gaussian about 0.5 (with a standard deviation of 0.01) to prevent a migration of the interface. The same constraint is imposed if chains are changed from one kind to the other in order to allow a fast equilibration of the minority component.[5] After having passed the tests for chain length and volume fraction ratio, the energy of the new state is compared to the energy of the old state and a Metropolis test is done.[6] If one of the three tests is not passed, the old state is retained. Although we have not explicitly established whether these rearrangements yield the correct ensemble averages, previous simulations have been encouraging in this respect.[1,3,4] Actually, the interface proved to be stable at $z = 0$ under the conditions chosen (sufficiently repulsive E_{AB}). Therefore it was not necessary to attach the chains of kind A to the wall at $z = -l_z/2$ and the B chains to the wall at $z = +l_z/2$. With this arrangement, accordingly, we have only the interface region and a continuous melt region. As a test, we carried out some simulations using ordinary periodic boundary conditions in the z direction, simulating a system with interfaces at $z = 0$ and $z = \pm l_z/2$. If l_z is chosen twice as large as in the previous arrangement, this arrangement is like simulating two systems that are periodically connected. The results are identical (not shown).

Calculational Details. For each lattice position the chain and segment number of the occupying chain segment and a code are stored. The code specifies how the next segment of the chain can be found and if the segment is an inner or an end segment. For each chain the end positions and its length are stored. For an end group reaction, an end segment and one of its neighboring lattice positions other than that occupied by the segment covalently bound to the end segment are chosen randomly and the rearrangement is attempted. For the metathesis a neighboring pair of segments is chosen randomly and the reaction is performed if possible. The ratio of selected end segments to the total number of selected segments is chosen such that metathesis reactions occur about as often as intermolecular rearrange-

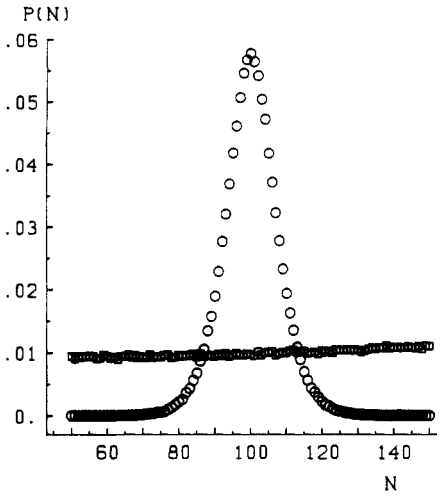

Figure 3. Chain length distribution, $P(N)$, of the majority component in the bulk region for $E_{AB} = 0.02$. (□) Constraint I, chains are constrained to fall into the interval $50 \leq N \leq 150$. (○) Constraint II, the chain length distribution narrowing technique by Olaj and Lantschbauer[3] is used with $f = 0.015$.

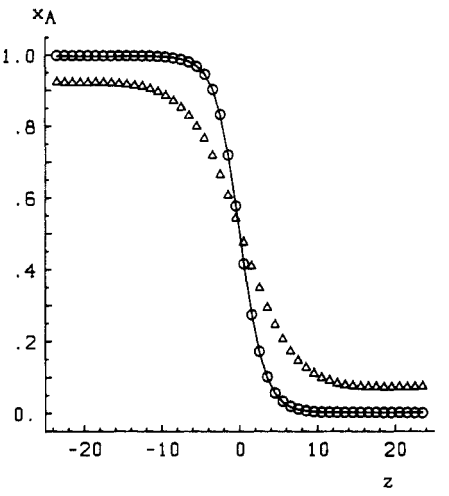

Figure 4. Volume fraction profile of A polymers at different z positions. Simulated data for $E_{AB} = 0.01$ (△) and $E_{AB} = 0.02$ (○), using constraint II. The connected line is a best fit of the data—calculated using $E_{AB} = 0.02$—according to the mean field theory.[9]

ments involving end segments. We equilibrated the system with more than 100 successful intermolecular rearrangements per segment and afterward measured chain properties every 0.02–0.2 attempted rearrangements per segment. More than 6000 such different data points were collected and averaged.

3. Results and Discussion

A critical point for all further investigations is the proper choice of the reduced interaction energy E_{AB}. With the quasichemical method[7] the critical decomposition energy is estimated to be roughly 0.005. A similar result is obtained with the Flory–Huggins theory;[8] i.e., $\chi_c = 2/N$, where $\chi = ZqE_{AB}$ is the Flory–Huggins parameter and Zq is the effective coordination number of a polymer segment. We have not attempted to determine the decomposition energy accurately since in this work we are interested in the structure of the interface at a repulsive energy sufficiently larger than the critical decomposition energy. Accordingly, we carried out our calculations with $E_{AB} = 0.02$, and in some cases also with $E_{AB} = 0.01$, both values clearly being in excess to $E_{AB} = 0.005$.

In Figure 3 we show the chain length distribution obtained with the two different constraints on chain lengths for $E_{AB} = 0.02$. The symmetric constraint (I) yields an almost rectangular distribution, as already noted by Madden.[1] The ratio of weight average to number average $\langle N^2\rangle/\langle N\rangle^2$ is 1.086 with a fraction of accepted rearrangements of about 0.1. On the other hand, with the Olaj–Lantschbauer constraint[3] (II) a quite narrow distribution of chain lengths is obtained, using a distribution-narrowing parameter of $f = 0.015$. In this case $\langle N^2\rangle/\langle N\rangle^2 = 1.006$ and the fraction of accepted rearrangements is about 0.05.

In Figure 4 the volume fraction profiles for the two different interaction energies of $E_{AB} = 0.01$ and $E_{AB} = 0.02$ are given for constraint II. The connected line is a best fit of the data at $E_{AB} = 0.02$ to the mean field profile[9] $x_A = 0.5 - (0.5 - x_{A0})\tanh(z/D)$, where x_A is the volume fraction of A at a given z position, x_{A0} is the volume fraction of A at minus infinity, and D is the thickness of the interface in lattice spacing units. The fitted data are $x_{A0} = 0.9970 \pm 0.0004$ and $D = 3.16 \pm 0.006$. Actually, the shape of the volume fraction profile at the interface is rather well described by the mean field solution that has been given by Cahn and Hilliard[9] for small molecules and by Helfand et al.[10,11] and by Leibler[12] for macromolecules. The broader distribution obtained under constraint I yields very similar profiles. The mutual miscibility of the two polymers, however, is slightly better and the interface is broader, i.e., $D = 3.28$ at $E_{AB} = 0.02$ (not shown). Experimentally found profiles[13] also agree very well with the shape of the mean field solution. As mentioned before, the thickness of the interface when fitted to our profile corresponds to 3.16 in lattice spacing units. With the formulas for the thickness given by Leibler, $D = 1/(9/2(\chi - 2/N))^{1/2}$, and Helfand et al., $D = 1/(6\chi)^{1/2}$, as quoted by Bates et al.,[13] who also discuss the two solutions, we calculate $D = 1.92$ and $D = 1.44$, respectively, where we assumed our mixture to be monodisperse and used again $\chi = ZqE_{AB}$. These mean field solutions underestimate the thickness of the interface considerably. Admittedly, an exact comparison is somewhat difficult. Thus, Sariban and Binder[14] have shown that the number of interactions is smaller than expected from mean field arguments. From a comparison of simulation results and mean field expressions, an "effective" interaction parameter χ_{eff} was calculated, which turned out to depend on composition.[14] As the mean field theories do not take into account the variation of the interaction parameter with composition, for this reason alone, a definite quantitative comparability of simulation results and mean field predictions is not warranted.

It might be also argued that the greater thickness obtained here is caused by the fact that we allow the ratio of A to B segments to fluctuate slightly about unity. This moderate fluctuation not only is necessary with our simulation method but also is even advantageous[5] because local equilibrium is reached faster. However, as further decrease of the standard deviation of these fluctuations does not change the thickness of the interface, these small fluctuations in A and B cannot be responsible for the deviation from mean field predictions.

In Figure 5 we show the number of nearest-neighbor heterocontacts per segment (NN) for $E_{AB} = 0.02$ and constraint II. This quantity is a measure of the local energy. It assumes its maximum at the interface. For comparison we have calculated this number also with the mean field theory:[7] $NN = x_A x_B Z q_A q_B/(q_A x_A + q_B x_B)$. Here Z (=6) is the coordination number of the lattice and Zq_A

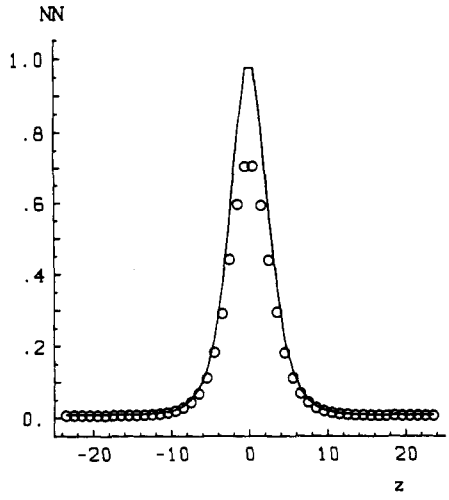

Figure 5. Average number of nearest-neighbor heterocontacts per segment, NN, for $E_{AB} = 0.02$, using constraint II: Simulated data (O) and mean field approximation by Guggenheim[7] (—).

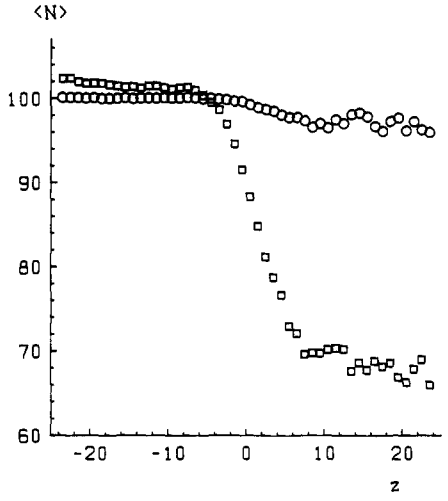

Figure 6. Profile of the number-average chain length, $\langle N \rangle$, for $E_{AB} = 0.02$, using constraint I (□) or constraint II (O). The average was determined from all A chains with their center of mass at a given z position and from B chains at the $-z$ position. Thus, left of interface the majority component is shown and on the right the minority component.

$= Z - 2 + 2/\langle N_A \rangle$ is the effective coordination number of a polymer segment (slightly larger than 4). The volume fractions of A and B segments, x_A and x_B, and the number-average chain lengths, $\langle N_A \rangle$ and $\langle N_B \rangle$, are calculated from the simulated data for every z position. The mean field solution is calculated only for the discrete values of z for which lattice data are available and these points are simply connected. It emerges that the mean field theory clearly overestimates the number of heterocontacts. The broad distribution (constraint I) yields very similar results but the number of heterocontacts is slightly larger (not shown).

It cannot be overlooked that—due to the more or less pronounced polydispersity of our system—a certain extent of "fractionation" occurs. The fraction of small chains is larger in the interface and in that phase where they form the minority component compared to the phase where they constitute the majority component, Figure 6. This effect is dramatic for the broad distribution (constraint I) but only small with the narrow distribution (constraint II). The polydisperse mixture therefore shows better miscibility. Similarly, we observe a large increase in the density of chain ends near the interface for the minority component, Figure 7. Necessarily, the opposite behavior is exhibited by the density of the centers of mass of the chains. Because of their higher number of degrees of freedom, the chain ends invade the other phase more readily than inner segments. This effect is particularly prominent with the narrow distribution (constraint II).

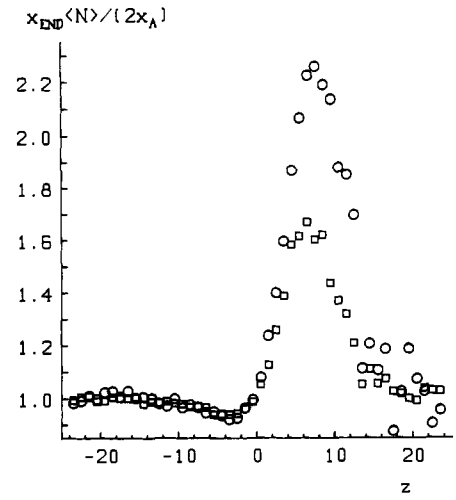

Figure 7. Relative amount of end segments for $E_{AB} = 0.02$, using constraint I (□) or constraint II (O). x_{END} is the volume fraction of chain ends, x_A is the volume fraction of A segments as shown in Figure 4, and $\langle N \rangle$ is the (position dependent) number-average chain length as shown in Figure 6. (For randomly distributed chain ends the plotted expression would be unity throughout.)

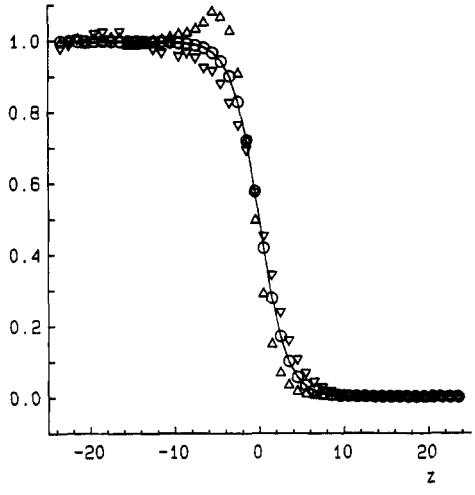

Figure 8. Density profiles—$E_{AB} = 0.02$, constraint II—of chain segments x_A (-O-), end segments $\langle N \rangle x_{END}/2$ (▽), and centers of mass $\langle N \rangle x_{COM}$ (△), where x_A is the volume fraction of A segments as shown in Figure 4 and x_{END} and x_{COM} are the volume fractions of end groups and centers of mass of A chains, respectively.

As a consequence, the density profiles of end segments and centers of mass should be different from the average segment density profile as shown in Figure 4. This is demonstrated in Figure 8 where all three profiles are superimposed for $E_{AB} = 0.02$ and constraint II. The slope at the interface is steepest for the centers of mass, while it is markedly smaller for the end groups. The overall segment profile shows an intermediate behavior. Accordingly, the evaluation of the thickness of the interface will yield different results depending on which profile actually is considered.

In Figure 9 we show the gyration radii in the x (or y) and z directions for the majority component chains under the same conditions. (The gyration radii of the minor-

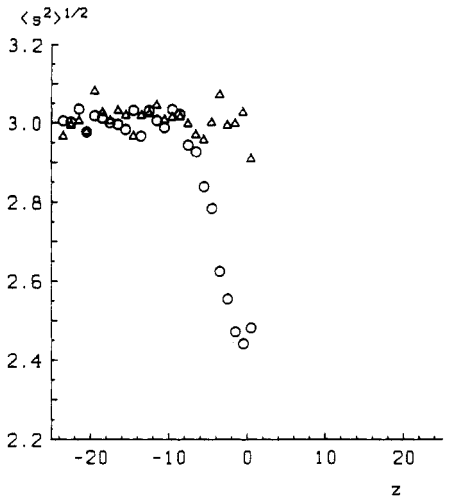

Figure 9. Profile of gyration radii for chains with a chain length of 100 taken from the narrow distribution (constraint II) for $E_{AB} = 0.02$: (Δ) component parallel to the interface, $[0.5\langle s_x^2 + s_y^2\rangle]^{1/2}$; (O) component perpendicular to the interface $\langle s_z^2\rangle^{1/2}$.

ity component are statistically too uncertain and are therefore omitted.) They are given for one chain length (N = 100) in order to avoid the problem of different average chain lengths at different z positions (we ignore those differences that occur because the chains are in a different environment with respect to average chain length and their distribution). At the interface the chains are compressed in the z direction while their dimensions in the x and y directions hardly change. Similar behavior is observed for the end-to-end distances and the scaling exponents (not shown). The same overall characteristics are exhibited also by chains taken from the broad distribution of chain length (constraint I).

4. Conclusions

The simulation of the interface region between two repulsive polymer melts is possible at a density of unity with pseudokinetic rearrangements if the ratio of A segments to B segments is forced to be narrowly distributed about unity. The interface or even several interfaces remain stable as chosen initially at any position (if E_{AB} is repulsive enough). However, with the constraint with respect to the position of the interface, we strongly believe that the interface and the melt take on an equilibrium configuration with meaningful local energies. With antiperiodic boundary conditions in the z direction we were able to avoid the need for a hard wall or a second interface.

It is very interesting to see how the system tries to take advantage of every inherent "degree of freedom" in order to lower the free energy at the interface. Thus, where shorter chains are available due to a broader chain length distribution, they are used to improve the miscibility and accordingly raise the entropy. If shorter chains are not present to an appreciable extent (as for constraint II), their role is mainly taken over by the chain ends. On the other hand, the coils apparently play their part by making the interface as smooth as possible, thus decreasing the energy at the interface. This is demonstrated by the behavior of those majority chains that are close to the interface, which exhibit a decrease of their dimensions perpendicular to the interface, which to some extent behaves like a repulsive wall. Of course, all these features are not independent of each other and partly may represent different aspects of the same basic processes.

Acknowledgment. We thank M. Wimmer for discussions.

References and Notes

(1) Madden, W. G. *J. Chem. Phys.* **1987**, *87*, 1405–1421.
(2) Olaj, O. F.; Lantschbauer, W.; Pelinka, K. H. *Chemie-Kunststoffe Aktuell* **1978**, *32*, 199.
(3) Olaj, O. F.; Lantschbauer, W. *Makromol. Chem., Rapid Commun.* **1982**, *3*, 847–858.
(4) Mansfield, M. L. *J. Chem. Phys.* **1982**, *77*, 1554–1559.
(5) Sariban, A.; Binder, K. *J. Chem. Phys.* **1987**, *86*, 5859–5873.
(6) Metropolis, N.; Rosenbluth, A. W.; Rosenbluth, M. N.; Teller, A. H.; Teller, E. *J. Chem. Phys.* **1953**, *21*, 1087–1092.
(7) Guggenheim, E. A. *Mixtures*; Clarendon Press: Oxford, 1952; pp 183–258.
(8) de Gennes, P.-G. *Scaling Concepts in Polymer Physics*; Cornell University Press: Ithaca, NY, 1979; p 106.
(9) Cahn, J. W.; Hilliard, J. E. *J. Chem. Phys.* **1958**, *28*, 258–267.
(10) Helfand, E.; Tagami, Y. *J. Chem. Phys.* **1972**, *56*, 3592–3601.
(11) Helfand, E.; Sapse, A. M. J. *J. Chem. Phys.* **1975**, *62*, 1327–1331.
(12) Leibler, L. *Macromolecules* **1982**, *15*, 1283–1290.
(13) Bates, F. S.; Dierker, S. B.; Wignall, G. D. *Macromolecules* **1986**, *19*, 1938–1945.
Sariban, A.; Binder, K. *Macromolecules* **1988**, *21*, 711–726.